

# Provenance and Tectonic Setting of the Permian Nam Duk Formation, North - Central Thailand: Implications for Geodynamic Evolution

Kitsana Malila<sup>a,b\*</sup>, Chongpan Chonglakmani<sup>b</sup>, Feng Qinglai<sup>c</sup>, and Dietrich Helmcke<sup>d</sup>

<sup>a</sup> PTT Exploration and Production Company Limited, PTTEP Office Building, 555 Vibhavadi Rangsit Rd., Chatuchak, Bangkok 10900, Thailand.

<sup>b</sup> School of Geotechnology, Institute of Engineering, Suranaree University of Technology, Nakhon Ratchasima, 30000 Thailand.

<sup>c</sup> Faculty of Earth Science, China University of Geosciences, Wuhan, 430074 P.R. of China.

<sup>d</sup> Goettinger Zentrum Geowissenschaften (GZG), D-37077 Goettingen, Germany.

\* Corresponding author, E-mails: KitsanaM@pttep.com and kitsana\_malila@hotmail.com

Received 23 Jul 2007

Accepted 9 Jan 2008

**ABSTRACT:** The Permian Nam Duk Basin is a part of the Phetchabun Fold Belt of central mainland Thailand. This basin is considered to be a geological backbone of tectonic evolution during the Late Paleozoic in Thailand. In this study, provenance analysis of the siliciclastic sediments of the Nam Duk Formation has been carried out based on geochemical and cathodoluminescence techniques. The geochemical result indicates that the siliciclastic sediment of Lower-Middle Permian "pelagic sequence" is a transitional deposit between an oceanic island arc and a continental island arc environments and is derived mainly from metabasic sources. During middle Middle to late Middle Permian, the provenance signatures of sandstones and shales from the "flysch" and the "molasse" sequences show indications of ultramafic-mafic igneous provenance and they were deposited in a continental island arc environment. The result supports the interpretation of Nan-Uttaradit ophiolitic belt north-west of the Nam Duk Basin as a major terrane which supplied siliciclastic sediments to the Nam Duk Basin during Middle-Late Permian.

**KEYWORDS:** Nam Duk Formation, Phetchabun Fold Belt, Provenance, Geodynamic Evolution.

## INTRODUCTION

The huge "Khorat Plateau" is bordered to the west by a belt of rock that reflects a complex Late Paleozoic to Quaternary history. It includes mountain ranges that stretch from the Mekong River in the north to Saraburi and Pak Chong in the south, a distance of approximately 400 km (Fig. 1). Known as the Loei Fold Belt<sup>1</sup>, it is located on the western margin of the Indochina plate. These N-S elongated mountain ranges are characterized by a series of different stratigraphic sequences and varying structural histories. Various researchers have studied the deformation history of the Loei or Phetchabun Fold Belt. The paleogeographic situation of the region during the Late Paleozoic time is still not clearly understood. Different scenarios have to be explored and it is expected that new data will provide a solution. This solution must be compatible with the wider geological interpretation of mainland SE Asia.

In this study, provenance analysis of the siliciclastic sediments of the Nam Duk Formation has been carried out based on geochemical and cathodoluminescence

(CL) techniques. The results can contribute significantly to a better understanding of the plate tectonic evolution of mainland Thailand during the Late Paleozoic.

## GEOLOGY AND STRATIGRAPHY

Based on Helmcke and Kraikhong<sup>2</sup> (1982), the stratigraphic succession of Permian Nam Duk Basin is composed of three units; pelagic facies, flysch facies and molasse facies related to pre-orogenic, syn-orogenic and post-orogenic events. These facies are exposed between milestone 16.00-20.20, 20.20-21.30, and 34.0-42.20 respectively on highway No. 12 from Lom Sak to Chum Phae.

According to Helmcke and Lindenberg<sup>3</sup> (1983), the first rock unit comprises mainly cherts, tuffs, shales, and allodapic limestones. The allodapic limestones were transported from south and north in the direction of the axis of the basin<sup>4</sup>. This facies represents a deep-sea basin depositional environment. The second rock unit consists of greywackes alternated with shales. In the greywackes all features of the Bouma-cycle can be found, characterizing them as turbidites. The third

rock unit comprises a very thick sequence of clastic rocks, mainly sandstones and shales. Some beds are very rich in fossil and plant remains. In the upper part of this section limestone layers are intercalated. These limestones are generally rich in foraminifers and sometimes contain corals. Towards the east the limestones become thicker and more prominent. The

foraminiferal fauna in the limestone is certainly autochthonous. The fauna are assigned to middle to late Middle Permian age<sup>5</sup>.

Winkel et al.<sup>4</sup> (1983) studied facies and stratigraphy of the lower Lower Permian strata of Phetchabun Fold Belt in central Thailand. They found that the turbiditic limestones (pelagic facies) were derived from

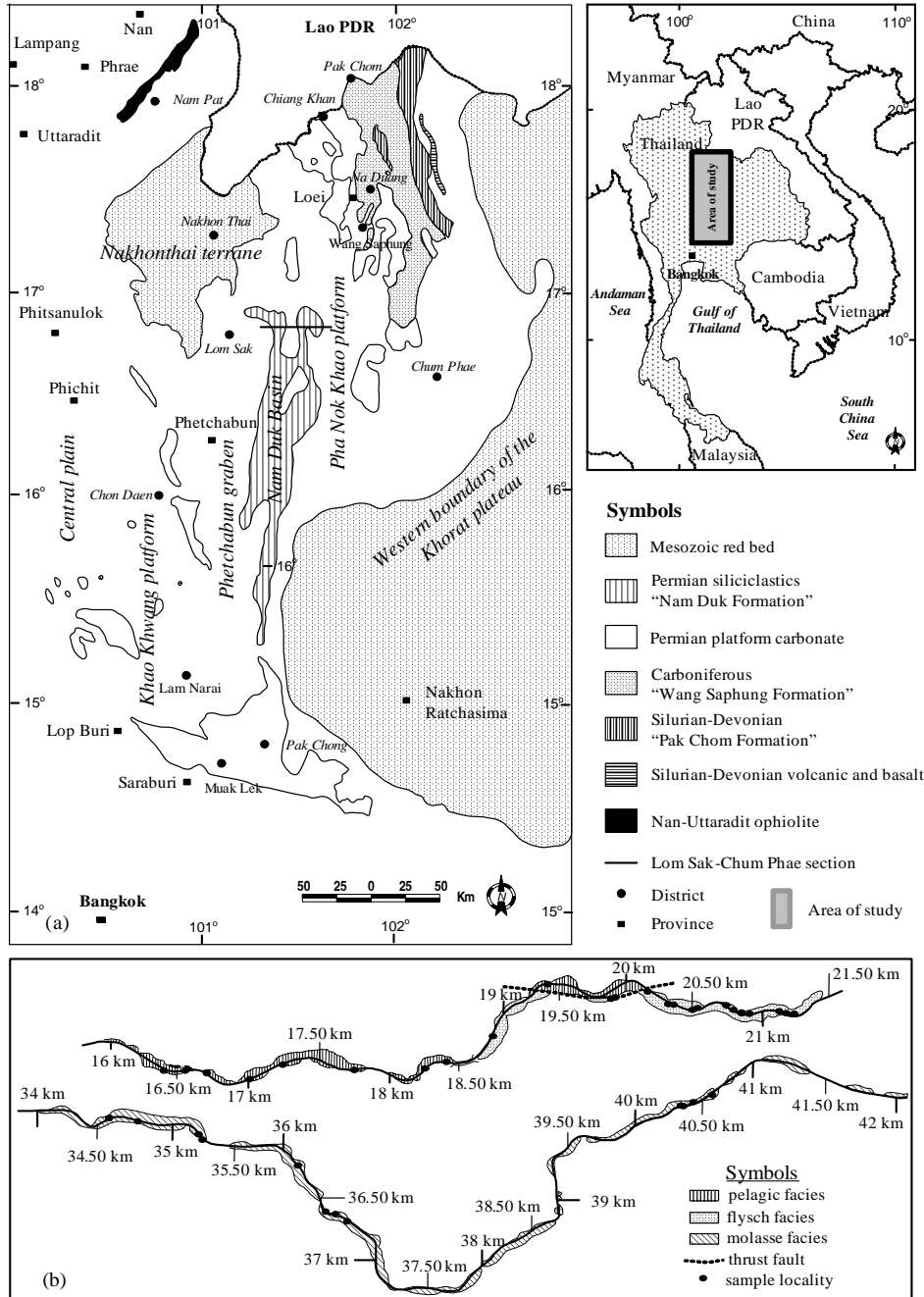


**Fig 1.** (a) Simplified geological map showing distribution of Late Paleozoic rock units and paleogeographic setting of the study area, west of the Khorat Plateau (modified from DMR, 1998). (b) Simplified geological map showing localities of collected samples from the Nam Duk Formation along highway No. 12 (modified from Helmcke et al., 1985). Sample numbers for geochemistry and cathodoluminescence analysis are indicated by milestone along the highway.

carbonate-platforms which are located in the eastern as well as in the western parts of the Phetchabun Fold Belt (Pha Nok Kao limestone of Chonglakmani and Sattayarak<sup>6</sup>, 1978 and Khao Khwang platform of Wielchowsky and Young<sup>7</sup>, 1985). They proved that the pelagic regime comprises the time interval of Upper Carboniferous? - Lower Permian to Lower Murgabian. Altermann et al.<sup>8</sup>(1983) proposed the timing of sudden onset of flysch sedimentation as an early Middle Permian. From paleontological data, they also proved

that the molasse sediments comprise not only Murgabian but also part of Midian, i.e. the molasse sedimentation prevailed into the middle-late Middle Permian. The study of fusulinoidean biostratigraphy by Charoentitirat<sup>9</sup> (2002) confirms that the molasse unit is in a Midian age.

Simplified geological map of the area bordering the Khorat Plateau to the west is shown in Figure 1. A paleogeographic map representing the Permian rock is shown in Figure 2.

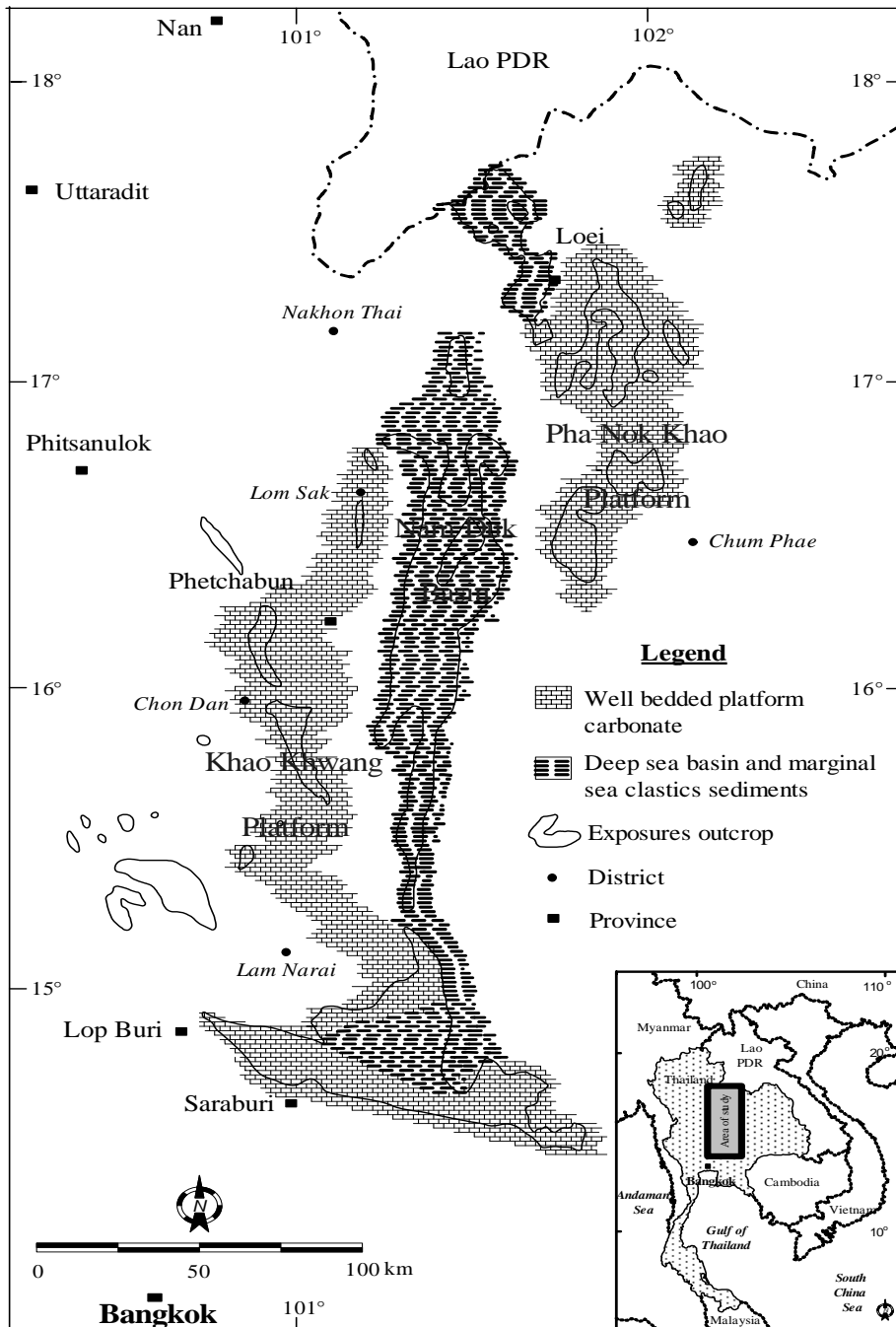


Fig 2. Permian non-restored paleogeographic map of Northeastern Thailand (Modified from Wielchowsky and Young, 1985).

## METHODOLOGY

Field work was carried out on the Nam Duk Formation during September, 2002 and February, 2003. Samples have been taken from type section of the Nam Duk Formation along the highway cut across the forestry area of the Phetchabun and Loei provinces. Sample localities in this paper are indicated by milestone numbers along highway No. 12 as shown in Figure 1. Samples were analyzed by geochemical and cathodoluminescence techniques. The results provided an interpretation for provenance and tectonic setting.

### Geochemical Analysis Technique

Geochemical analyses were performed for major and trace elements. The samples were crushed and splitted before grinding and sieving for powder. Thirty samples of sandstone and shale of flysch and molasse sequences were analyzed for major elements by high resolution X-ray fluorescence analysis (Energy Dispersive Spectrometer, Oxford-Model ED-2000) at the laboratory of Suranaree University of Technology. The procedure, accuracy, reproducibility and lower limit of detection are reported in several publications. Thirty three samples of sandstone, shale, and allodapic limestone of all sequences were analyzed for trace element and rare earth elements by inductively coupled plasma mass spectrometry (ICPMS) at the Key Laboratory of the Lithosphere and Crustal Evolution, China University of Geosciences (Wuhan). Detection limits ranged from 0.003-0.1  $\mu\text{g g}^{-1}$  for heavier mass elements to 0.01-1  $\mu\text{g g}^{-1}$  for lighter mass elements. Major elements comprise  $\text{SiO}_2$ ,  $\text{TiO}_2$ ,  $\text{Al}_2\text{O}_3$ ,  $\text{Fe}_2\text{O}_3$ ,  $\text{MnO}$ ,  $\text{MgO}$ ,  $\text{CaO}$ ,  $\text{Na}_2\text{O}$ ,  $\text{K}_2\text{O}$ ,  $\text{P}_2\text{O}_5$ , and  $\text{SO}_3$ . Trace elements including rare earth elements comprise Sc, V, Cr, Co, Ni, Cu, Zn, Ga, Rb, Sr, Zr, Mb, Mo, Cd, Cs, Ba, La, Ce, Pr, Nd, Sm, Eu, Gd, Tb, Dy, Ho, Er, Tm, Yb, Lu, Hf, Ta, Pb, Th, and U. The geochemical analysis result is presented by Malila<sup>10</sup> (2005).

Several studies including Bhatia<sup>11</sup> (1983) and Roser and Korsch<sup>12</sup> (1986) led to the recognition of major elements as useful discriminating parameters. The discrimination diagram for sandstone, based upon a bivariate plot of  $\text{TiO}_2$  and  $(\text{Fe}_2\text{O}_3 + \text{MgO})$ , was proposed by Bhatia<sup>11</sup> (1983). The fields display oceanic island arc, continental island arc, active continental margin, and passive margin environments of deposition. Tectonic-setting discrimination diagrams using  $\text{K}_2\text{O}/\text{Na}_2\text{O}$  ratio and  $\text{SiO}_2$  content are applied<sup>12</sup>. The diagrams are suitable for sandstone-mudstone and show the field of a passive continental margin, an active continental margin and an island arc environment of deposition. Ti and Al are generally considered to be chemically immobile constituents of weathering profiles, sediments and sedimentary rocks<sup>13</sup>, and may

be used as provenance indicators<sup>14</sup>. The  $\text{TiO}_2$  versus  $\text{Al}_2\text{O}_3$  plot showing fields of alkali granite, granodiorite, and peridotite provenance is presented. A discrimination function diagram has been proposed by Roser and Korsch<sup>15</sup> (1988) to distinguish between sediments whose provenance are primarily mafic, intermediate or felsic igneous and quartzose sedimentary rocks. A plot of two discriminate functions, based upon the oxides of Ti, Al, Fe, Mg, Ca, Na, and K, differentiates most effectively the four provenances.

Trace elements, concentrations of trace element and their ratios can be useful discriminators of tectonic settings because some trace elements are considered to be immobile during sedimentation<sup>16</sup>. A simple two-component mixing model (ratio-ratio plots Co/Th vs La/Sc, Co/Th vs Sc/Th) using incompatible and compatible elements are plotted. The ferromagnesian trace elements, Ni, Cr, and V are generally abundant in mafic and ultramafic rocks, and their enrichment in sedimentary rocks may be indicative of the presence of these rocks in the provenance area<sup>17</sup>. The abundance of mafic and ultramafic rocks in the provenance can be further tested by Y/Ni ratios. Cr/V ratios can also indicate the presence of chromite among the heavy minerals<sup>17</sup>.

The amount of La, Th, Ba, Sc, Co, Cr and their element ratios such as La/Sc, Th/Sc, Ba/Sc, La/Cr, Th/Cr are useful indicators discriminating basic and felsic source rocks<sup>18,19,20</sup>. The immobile elements have also been used for the same purpose as major elements. In general, there is a systematic increase in the light rare-earth elements (La, Ce, and Nd), in Th and Nb, and in a La/Y ratio; and a decrease in V and Sc in greywackes from oceanic island arc to continental island arc, to active continental margin, and to passive continental margin. The trace elements discriminators of tectonic settings and source composition of Nam Duk Formation are compared to the study of Bhatia and Crook<sup>16</sup> (1986) and Culler<sup>20</sup> (1994). Distinctive fields for four environments; oceanic island arc, continental island arc, active continental margin and passive margin are recognized on the ternary plots of La-Th-Sc, Th-Sc-Zr/10 and Th-Co-Zr/10. However, on a La-Th-Sc plot, the fields of active continental margin sediments and passive margin sediments are overlapped, but the Th-Sc-Zr/10 shows distinct separation.

### Cathodoluminescence (CL) Technique

The samples used for CL measurement are performed on an extremely smooth, highly polished and carbon-coated thin section to prevent charging under electron bombardment. A commercially produced hot-cathodoluminescence microscope (HCL-LM) after Neuser et al.<sup>21</sup> (1995) is provided with high-vacuum chamber ( $< 10^{-5}$ ) and uses acceleration

voltage of 14 KeV. The CL instruments and thin sections preparation were done at the Center of Geosciences, University of Göttingen, F. R. Germany during 2003-2005.

The CL color of quartz and feldspar in sandstone may provide a signature of the source rock from which individual grains, or populations of grains, were derived. This information, in concert with conventional

petrography, study of accessory minerals, and geochemistry, provided a broad base upon which to infer petrogenetic relations (such as shared source regions), provenance, and to some extent, paleotectonic setting<sup>22</sup>.

Zinkernagel<sup>23</sup> (1978) defined three types of quartz, based on CL and original occurrence as follow: *violet-luminescing quartz*, from plutonic, volcanic, and contact

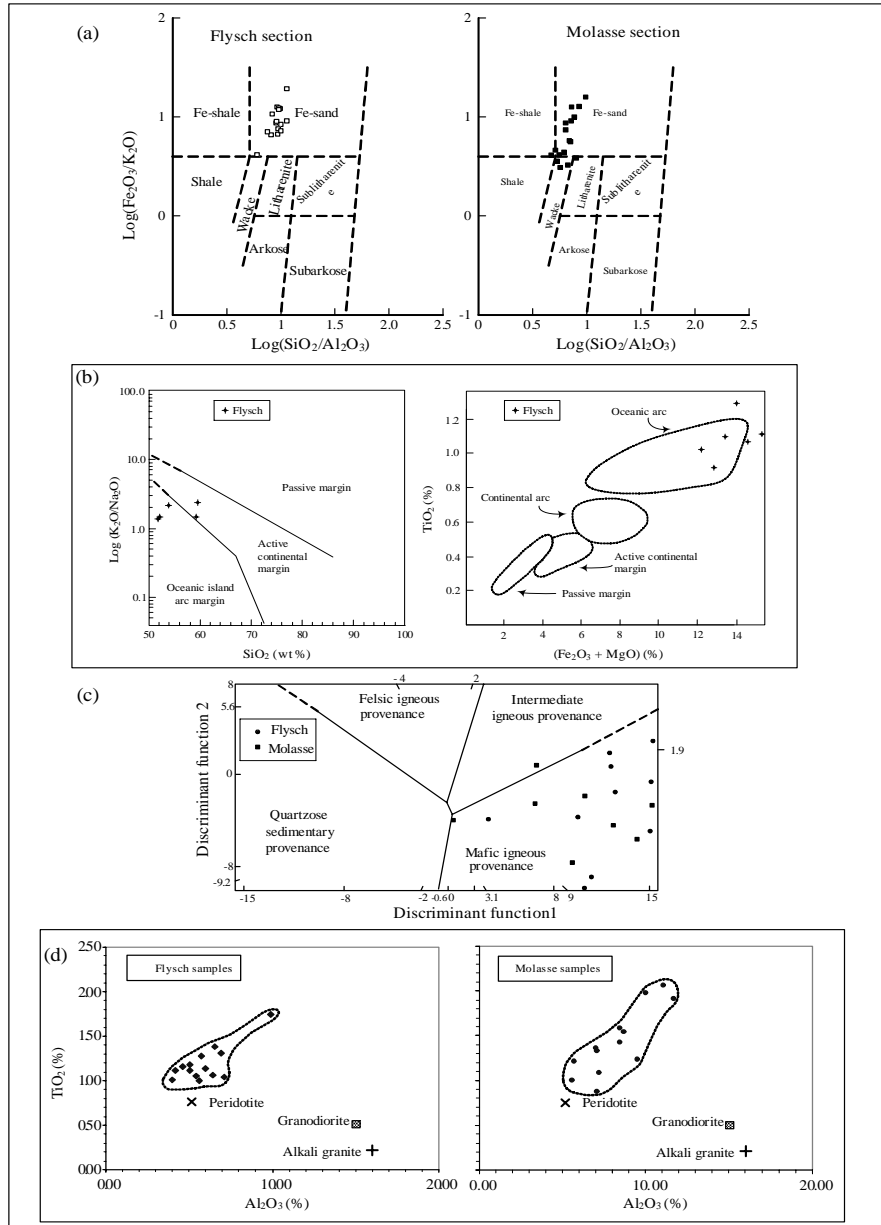


**Fig 3.** (a) Classification of terrigenous sandstones and shales of flysch and molasse samples (after Herron, 1988). The plots fall into the field of Fe-sand in flysch and Fe-sand and Wacke in molasse samples. (b) Discrimination diagram of Roser and Korsch (1986) for flysch samples showing the field of oceanic island arc margin to active continental margin and diagram for flysch samples based upon a bivariate plot of  $\text{TiO}_2$  versus  $(\text{Fe}_2\text{O}_3 + \text{MgO})$  (Bhatia, 1983). (c) Provenance signature of flysch and molasse siliciclastic sediments using major elements indicates mafic igneous source of flysch and molasse samples (modified from Roser and Korsch, 1988). (d)  $\text{TiO}_2$  versus  $\text{Al}_2\text{O}_3$  plot for the flysch and molasse samples shows a positive correlation trend with peridotite end member (Young and Nesbitt, 1998).

metamorphic rocks or rocks which have undergone fast cooling; *brown-luminescing quartz*, from low-grade metamorphic rocks, or from high-grade metamorphic rocks which have been slowly cooled; and *nonluminescing quartz*, from authigenic process. The recent general classification of the CL behavior of the CL detrital quartz<sup>24</sup> distinguishes the following criteria: *blue or violet*, plutonic quartz as well as quartz phenocrysts in volcanic rocks, and high grade metamorphic quartz; *red*, matrix quartz in volcanic rocks; *brown*, quartz from regional metamorphic rocks; *non or weakly luminescent*, authigenic quartz; *short-lived green or blue*, hydrothermal and pegmatitic quartz.

Müller<sup>25</sup> (2000) studied CL properties of magmatic quartz and has subdivided it into (1) euhedral quartz phenocrysts showing stable, dominantly blue CL and growth zoning related to Ti distribution and (2) anhedral matrix quartz with unstable red-brown CL and homogeneous trace element distribution. Rhyolitic and granitic quartz phenocrysts also show similar growth textures. Hydrothermal quartz shows similar growth patterns as magmatic quartz, but stepped zoning is dominant. The application of scanning cathodoluminescence (SEM-CL) imaging to characterize volcanic, plutonic, and metamorphic quartz was proposed<sup>26,27</sup>. According to Seyedolali et al.<sup>26</sup> (1997), the volcanic quartz is characterized by well-developed zoning in CL images. Plutonic quartz may also be zoned, but much plutonic quartz is unzoned. Metamorphic quartz is more complex; its

characteristics depend upon whether metamorphism has been largely thermal (contact metamorphism) or has resulted from regional tectonic forces. Thermally metamorphosed quartz typically displays few internal features in CL images, other than a few late-stage fractures, or it has a kind of indistinct, ill-defined, mottled texture.

## RESULT

### Geochemistry

#### Major Elements

According to Herron<sup>28</sup> (1988), the  $Fe_2O_3/K_2O$  ratio is more successfully classified shale and sandstone. In term of the  $SiO_2/Al_2O_3$  and  $Fe_2O_3/K_2O$  ratios, the siliciclastic samples are plotted and display type of terrigenous siliciclastic sediments. All the flysch samples fall in the field of Fe-sand in the plots of  $SiO_2/Al_2O_3$  and  $Fe_2O_3/K_2O$  (Fig. 3a). The samples of molasse sequence are scattered and fall similarly into the field of Fe-sand with some in Wacke (Fig 3a). Both sequences have very high  $TiO_2$  and  $Fe_2O_3$ , but low  $Al_2O_3$ , and a wide range of CaO and  $K_2O$ . However, an average concentration of  $TiO_2$ ,  $Fe_2O_3$ , and  $Al_2O_3$  of flysch samples are lower than molasse samples. It seems to be less  $Na_2O$  content in molasse samples, only a few ppm (two samples) can be detected.

The tectonic-setting discrimination diagram using  $K_2O/Na_2O$  ratio and  $SiO_2$  content<sup>12</sup> was applied to flysch and molasse sequences. Due to small  $Na_2O$  content in

**Table 1.** Standard sedimentary compositions and Permian siliciclastic sediments from the Nam Duk Formation including Nan-Uttaradit suture zone used for normalizing the REE concentration in sedimentary rocks (in ppm).

| REE        | NASC<br>1     | PAAS<br>2     | Upper crust<br>3 | ES<br>4       | Pelagic<br>5 | Flysch<br>6  | Molasse<br>7  | Chert, Nan<br>8 |
|------------|---------------|---------------|------------------|---------------|--------------|--------------|---------------|-----------------|
| La         | 31.10         | 38.20         | 30.00            | 41.10         | 19.29        | 20.83        | 24.62         | 2.17            |
| Ce         | 67.03         | 79.60         | 64.00            | 81.30         | 33.08        | 36.88        | 46.20         | 2.97            |
| Pr         |               | 8.83          | 7.10             | 10.40         | 5.00         | 5.02         | 5.95          | 0.48            |
| Nd         | 30.40         | 33.90         | 26.00            | 40.10         | 20.47        | 18.39        | 22.19         | 1.79            |
| Sm         | 5.98          | 5.55          | 4.50             | 7.30          | 4.81         | 3.71         | 4.53          | 0.50            |
| Eu         | 1.25          | 1.08          | 0.88             | 1.52          | 1.05         | 0.81         | 1.00          | 0.16            |
| Gd         | 5.50          | 4.66          | 3.80             | 6.03          | 4.45         | 3.23         | 4.01          | 0.41            |
| Tb         | 0.85          | 0.77          | 0.64             | 1.05          | 0.77         | 0.54         | 0.69          | 0.08            |
| Dy         | 5.54          | 4.68          | 3.50             |               | 4.21         | 3.03         | 3.86          | 0.40            |
| Ho         |               | 0.99          | 0.80             | 1.20          | 0.87         | 0.60         | 0.77          | 0.09            |
| Er         | 3.28          | 2.85          | 2.30             | 3.55          | 2.24         | 1.68         | 2.11          | 0.28            |
| Tm         |               | 0.41          | 0.33             | 0.56          | 0.33         | 0.25         | 0.33          | 0.04            |
| Yb         | 3.11          | 2.82          | 2.20             | 3.29          | 2.32         | 1.78         | 2.28          | 0.28            |
| Lu         | 0.46          | 0.43          | 0.32             | 0.58          | 0.39         | 0.29         | 0.37          | 0.04            |
| <b>Sum</b> | <b>154.50</b> | <b>184.77</b> | <b>146.37</b>    | <b>197.98</b> | <b>99.28</b> | <b>97.04</b> | <b>118.91</b> | <b>9.70</b>     |

1 North American shale composite (Gromet et al., 1984)

2 Post Archaean average Australian sedimentary rock (McLennan, 1981)

3 Average upper continental crust (Taylor and McLennan, 1981)

4 Average European shale (Haskin and Haskin, 1966)

5 Average Pelagic sequence of the Nam Duk Formation (this study)

6 Average Flysch sequence of the Nam Duk Formation (this study)

7 Average Molasse sequence of the Nam Duk Formation (this study)

8 Permian "Chert" from Nan-Uttaradit Ophiolitic sequence (Malila, 2005)

**Table 2.** Trace element discriminators of tectonic settings and source composition.

| Trace ele.   | Graywackes, Bhatia and Crook (1986) |                           |                        |                    | Culler (1994)                   |                                | Nam Duk Formation(this study) |              |               |
|--|-------------------------------------|---------------------------|------------------------|--------------------|---------------------------------|--------------------------------|-------------------------------|--------------|---------------|
|  | Passive margin                      | Active continental margin | Continental island arc | Oceanic island arc | high-silica metamorphic sources | low-silica metamorphic sources | Molasse (ave)                 | Flysch (ave) | Pelagic (ave) |
| <b>Discriminators decreasing toward oceanic island or low silica sources</b> |                                     |                           |                        |                    |                                 |                                |                               |              |               |
| Pb   | 16.00                               | 24.00                     | 15.10                  | 6.90               |                                 |                                | 14.99                         | 12.18        | 11.11         |
| Th   | 16.70                               | 8.80                      | 11.10                  | 2.27               | 17.00                           | 8.00                           | 9.40                          | 6.88         | 3.50          |
| Zr   | 298.00                              | 179.00                    | 229.00                 | 96.00              |                                 |                                | 210.36                        | 185.98       | 159.35        |
| Hf   | 10.10                               | 6.80                      | 6.30                   | 2.10               | 12.20                           | 6.90                           | 6.08                          | 5.26         | 4.66          |
| Nb   | 7.90                                | 10.70                     | 8.50                   | 2.00               |                                 |                                | 9.44                          | 7.58         | 6.47          |
| La   | 33.50                               | 33.00                     | 24.40                  | 8.72               | 57.00                           | 45.50                          | 24.62                         | 20.83        | 33.98         |
| Ce   | 71.90                               | 72.70                     | 50.50                  | 22.53              | 127.00                          | 87.00                          | 46.20                         | 36.88        | 54.86         |
| Nd   | 29.00                               | 25.40                     | 20.80                  | 11.36              |                                 |                                | 22.19                         | 18.39        | 35.37         |
| Rb/Sr  | 1.19                                | 0.89                      | 0.65                   | 0.05               |                                 |                                | 0.353                         | 0.133        | 0.078         |
| La/Y   | 1.31                                | 1.33                      | 1.02                   | 0.48               |                                 |                                | 1.134                         | 1.188        | 0.757         |
| La/Sc  | 6.25                                | 4.55                      | 1.82                   | 0.55               | 20.00                           | 1.80                           | 2.484                         | 2.584        | 1.598         |
| Th/Sc  | 3.06                                | 2.59                      | 0.85                   | 0.15               | 7.00                            | 0.33                           | 0.949                         | 0.854        | 0.285         |
| Th/U   | 5.60                                | 4.80                      | 4.60                   | 2.10               |                                 |                                | 4.159                         | 3.865        | 2.340         |
| Ba/Sc  |                                     |                           |                        |                    | 268.00                          | 29.50                          | 19.037                        | 17.019       | 10.557        |
| La/Cr  |                                     |                           |                        |                    | 3.70                            | 0.98                           | 0.029                         | 0.023        | 0.116         |
| Th/Cr  |                                     |                           |                        |                    | 1.10                            | 0.11                           | 0.011                         | 0.008        | 0.021         |
| <b>Discriminators increasing toward oceanic island or low silica sources</b> |                                     |                           |                        |                    |                                 |                                |                               |              |               |
| Ti   | 0.22                                | 0.26                      | 0.39                   | 0.48               |                                 |                                |                               |              |               |
| Sc   | 6.00                                | 8.00                      | 14.80                  | 19.50              | 4.50                            | 31.00                          | 9.910                         | 8.060        | 12.070        |
| Co   | 5.00                                | 10.00                     | 12.00                  | 18.00              |                                 |                                | 13.700                        | 14.250       | 11.470        |
| Zn   | 26.00                               | 52.00                     | 74.00                  | 89.00              |                                 |                                | 67.990                        | 59.440       | 65.380        |
| Cr   |                                     |                           |                        |                    | 18.50                           | 113.00                         | 840.760                       | 899.050      | 166.890       |
| Ti/Zr  | 6.74                                | 15.30                     | 19.60                  | 59.80              |                                 |                                |                               |              |               |
| Zr/Hf  | 29.50                               | 26.30                     | 36.30                  | 45.70              |                                 |                                | 34.599                        | 35.357       | 36.342        |
| Zr/Th  | 19.10                               | 9.50                      | 21.50                  | 48.00              |                                 |                                | 22.379                        | 27.029       | 29.052        |
| La/Th  | 2.20                                | 1.77                      | 2.36                   | 4.26               |                                 |                                | 2.619                         | 3.028        | 5.608         |

molasse sequences, only the data obtained from flysch sequence are plotted. They show indication of an oceanic island arc margin to active continental margin setting (Fig. 3b). The discrimination, based upon a bivariate of  $TiO_2$  and  $(Fe_2O_3 + MgO)$  are plotted. Due to the high  $TiO_2$  content, only half of samples from flysch sequence can be plotted and they fall into the field of an oceanic arc setting (Fig. 3b). The provenance signatures of siliciclastic sandstones from flysch and molasse are plotted by using discrimination diagram of Roser and Korsch (1988). Scattering plots of both sequences show dominantly mafic igneous provenance (Fig. 3c). The best-fit line of the  $TiO_2$  versus  $Al_2O_3$  of flysch and molasse passes through the estimated peridotite end member which indicates an ultramafic-mafic provenance<sup>14</sup> (Fig. 3d).

#### Trace Elements

In the pelagic sequence, shales and micritic-limestones have been chosen for samples. As for flysch and molasse sequences, sandstones and shales are more prominent and are used for trace elements analysis. Cr/V ratios of flysch and molasse samples are higher than 1 which indicates the presence of chromite among the heavy mineral during deposition<sup>29</sup>. The high Cr/V ratio may indicate that the influence of diagenetic

factors as a result of anoxic bottom-water conditions during deposition was not significant enough to enrich the vanadium. Y/Ni ratios in the flysch and molasse are low which confirms that the mafic and ultramafic rocks were abundantly present in the source area of the Nam Duk Formation<sup>29</sup>.

Chondrite normalized REE and trace elements abundance patterns of pelagic, flysch, and molasse samples are compared with the sedimentary composition standard as shown in Table 1. Comparison of REE plot from well known source and the Nam Duk Formation including chert sample from Nan-Uttaradit Suture Zone is studied by Malila<sup>10</sup> (2005). Summation of rare earth elements increases from an oceanic island arc to a continental island arc, and it is the highest in an Andean-type margin and a passive margin<sup>30</sup>. Summation of REE of the flysch is higher than molasse and is nearly the same as pelagic samples. In addition, these values are also less than the average summation of REE from North American shale composite (NASC), post Archaean average Australian shale (PAAS), Upper Crust, and European shale. The result indicates that the Nam Duk Basin was not derived from the Upper Crust and should have been deposited in the oceanic to continental island arc environments.

According to the comparison data in Table 2, the flysch and molasse samples show similarity of a continental island arc setting<sup>16</sup> and indicate low-silica metamorphic sources<sup>20</sup>. Pelagic samples are not clearly defined. They show values between an oceanic to a

continental island arc setting and indicate low-silica metamorphic sources. A La-Th-Sc and Th-Sc-Zr/10 ternary diagrams are plotted to discriminate tectonic setting and composition of source rocks as shown in Figure 4<sup>16,20</sup>. However, on a La-Th-Sc plot, the fields of

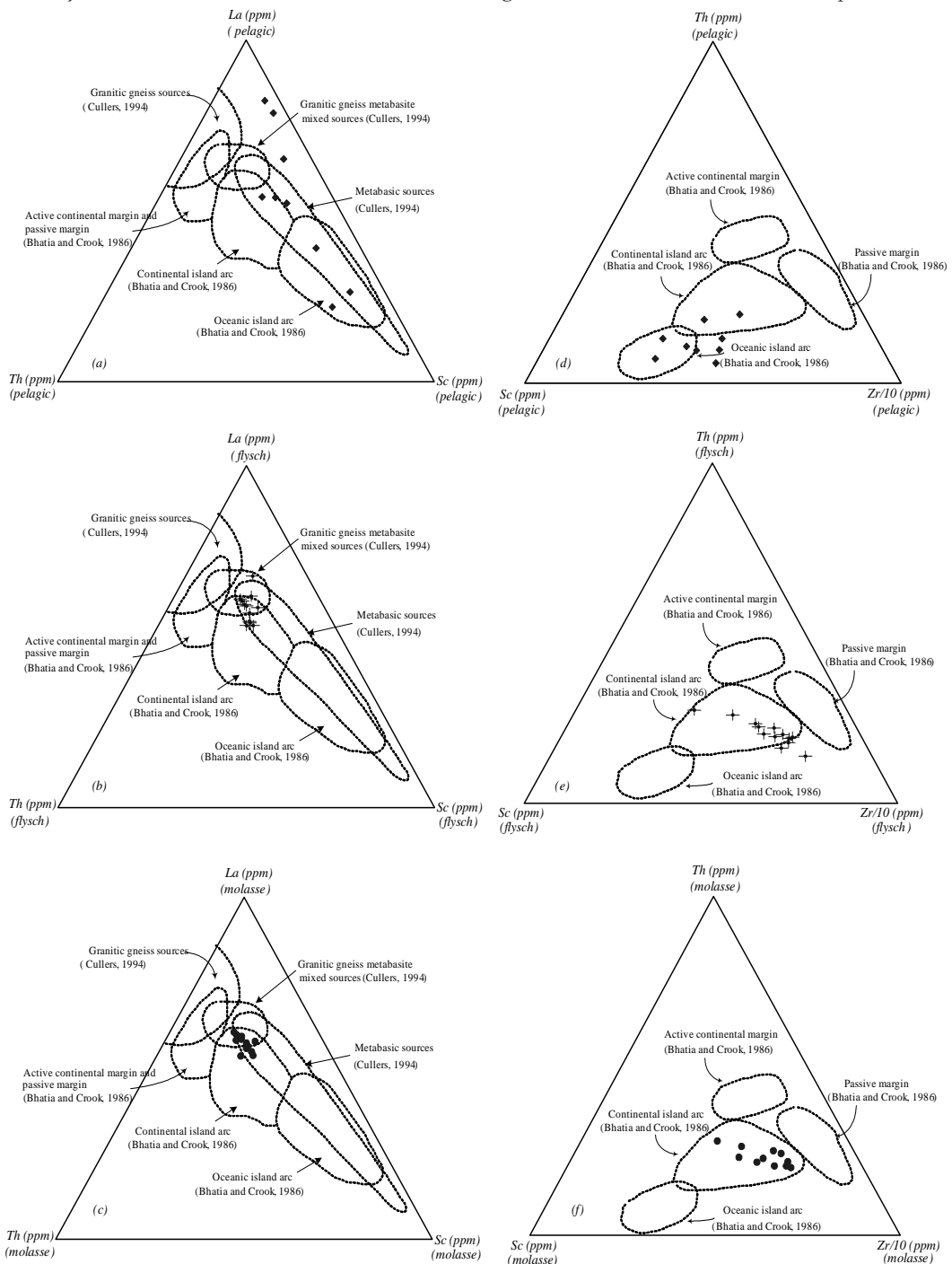


**Fig 4.** La-Th-Sc ternary diagram for pelagic (a), flysch (b), and molasse (c) siliciclastic sediments of the Nam Duk Formation (after Bhatia and Crook, 1986; Cullers, 1994). Th-Sc-Zr/10 ternary diagram for pelagic (d), flysch (e), and molasse (f) siliciclastic sediments of the Nam Duk Formation (after Bhatia and Crook, 1986). Explanation of tectonic setting and provenance are shown in each figure.

active continental margin and passive margin sediments are overlapped, but the Th-Sc-Zr/10 shows distinct separation. For pelagic sequence, the result of a La-Th-Sc ternary diagram plot falls into the field of an oceanic island arc and a continental island arc setting and they

were derived mainly from metabasic source. The sediments of flysch and molasse sequences are derived from mixed sources from metabasic and granitic gneiss and fall into the field of a continental island arc setting. In consideration of the Th-Sc-Zr/10 plots, most of

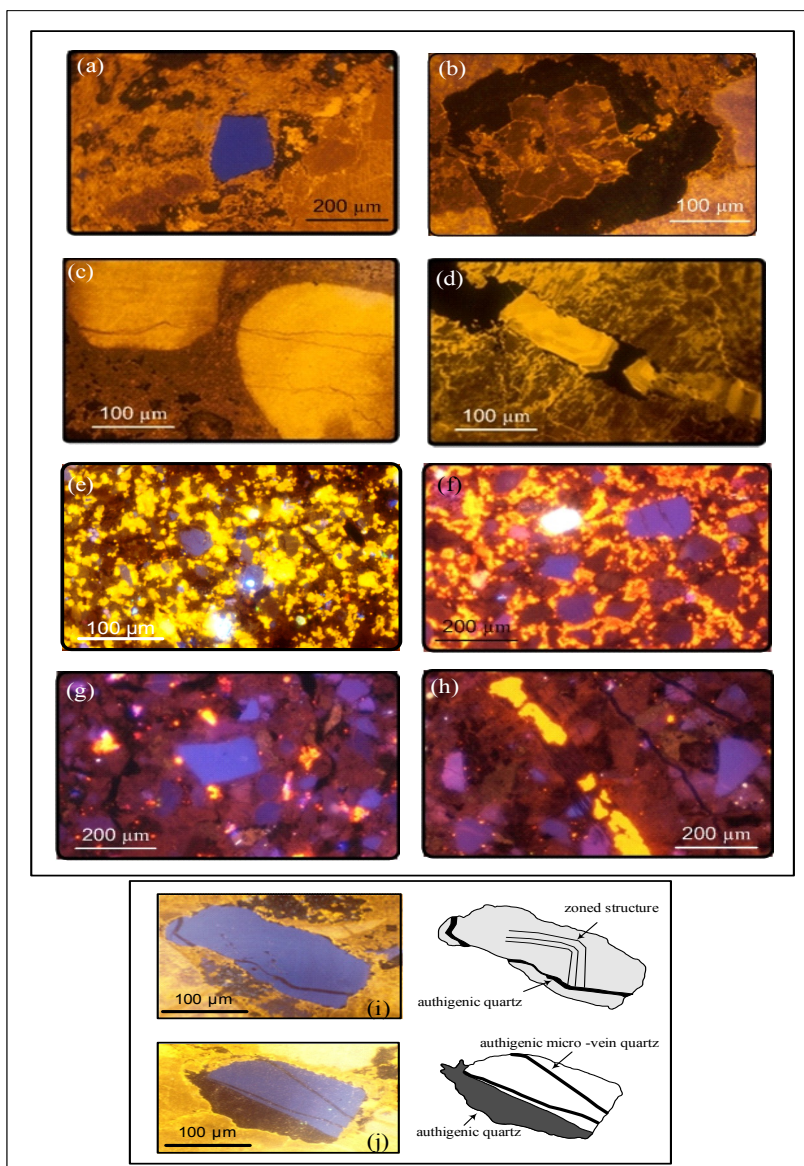


**Fig 5.** (a) CL micrograph of pelagic sample no. 17+100 displays volcanic (blue CL) detrital quartz in the allodapic limestone. (b) CL micrograph of pelagic sample no. 17+120 displays a bright zone containing  $Mn^{2+}$  activator; and a dark zone more or less free of  $Mn^{2+}$  and  $Fe^{2+}$ , indicating at least second phase of diagenesis. (c) CL micrograph of pelagic sample no. 17+120 displays micro-veins of sparitic calcite texture which are well identified by CL image and not evident in ordinary light. (d) CL micrograph of pelagic sample no. 17+127 displays an opaque mineral in a younger calcite vein. (e) CL micrograph of flysch sample no. 18+720 displays calcite cementation with mainly fine-grained brown and minor blue CL quartz. (f) CL micrograph of flysch sample no. 20+375 displays calcareous cementation with violet, blue and brown CL quartz. (g) CL micrograph of flysch sample no. 20+550 displays authigenic quartz cement (dark CL image) and mainly brown and blue CL quartz and carbonate (yellow) grains. (h) CL micrograph of flysch sample no. 21+050 displays authigenic siliceous cement with younger calcite and authigenic quartz veins and mainly brown and blue CL quartz. (i) deformed detrital volcanic quartz in allodapic limestone of sample No. 17+100 displays blue CL with zoned feature and healed authigenic quartz. (j) Overgrowth of authigenic quartz in volcanic quartz grain of sample No. 17+120.

pelagic samples fall into the fields of an oceanic island arc and a continental island arc setting. On the contrary, only the field of a continental island arc setting is plotted in flysch and molasse sequences. This result is consistent with the low La, Th, U, Zr, and Nb concentrations in the sandstones and shales.

### Cathodoluminescence

The allodapic limestone samples were collected from pelagic sequence. Sample numbers indicate milestone at the sampling locality along highway No. 12. Thin sections under ordinary light and cathodoluminescence are given in Figure 5 and Figure 6. In general,

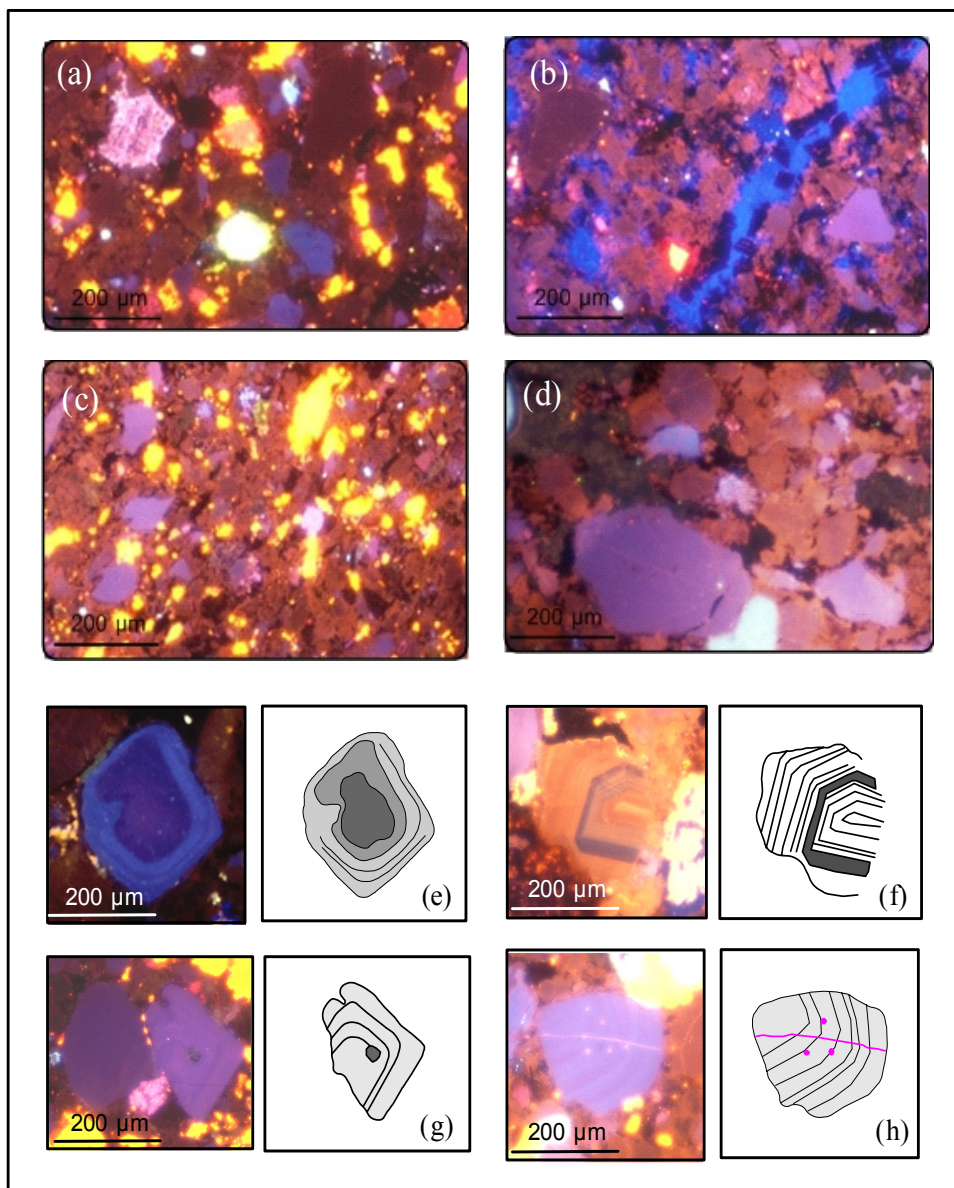


**Fig 6.** (a) CL micrograph of molasse sample no. 34+750. Browned quartz grains are dominant in the rock with some carbonate grains. A few coarse quartz are blue and light purple. (b) CL micrograph of molasse sample no. 35+175. Browned quartz grains are dominant in the rock. A few quartz grains are dark blue and moderate feldspar grains are scattered in the figure. (c) CL micrograph of molasse sample no. 36+650. Fine-grained brown quartz is dominant in the rock with some carbonate grains. A few coarse quartz grains are blue and pinkish blue. (d) CL micrograph of molasse sample no. 37+550. Browned quartz grains are dominant in the rock. A few coarse quartz grains are blue with streak feature. (e) Quartz in molasse sample no. 40+400 displays stepped zoning from violet-light blue-dark blue. (f) Quartz zoning in molasse sample no. 40+400 displays growth sector with light reddish brown, light purple, violet, and light reddish brown. (g) Quartz zoning in molasse sample no. 34+750 displays stepped zoning of light purple with non luminescent defect near the center. (h) Quartz zoning in molasse sample no. 34+750 displays stepped zoning of light blue with pinkish point and micro-vein.

photomicrographs of all samples show skeletal fragments of crystalline packstone. Some foraminifera (fusulinid), deformed quartz and feldspar can be observed. Thin-section under CL shows syn-sedimentary elements such as clastic and biogenic components. The alteration rim of calcite and quartz grains with overgrowth of authigenic quartz is well observed. Micro-vein which is invisible from ordinary light and younger calcite vein (growth zonation) with opaque mineral are well developed. Most of the quartz grains show typical blue color and some grains were deformed before deposition. A zoned structure of blue luminescence quartz with an authigenic vein is clearly shown in Figure 5. In addition, fine-grained crystalline quartz texture is represented by dark brown luminescence. As mentioned above, the detrital quartz grains from the allodapic limestone of the pelagic sequence displayed by blue CL indicate the volcanic and plutonic sources. The presence of brown crystalline quartz indicates derivation from Low-T hydrothermal influence.

The result of detrital quartz CL in flysch sequence shows brown and blue color (Fig. 5). Detrital quartz grains of sample no. 18+720 (lower part of flysch sequence) show mainly brown color and some of them display crystalline texture. They indicate a regional low-grade metamorphic provenance. Blue CL quartz grains are increasing and more prominent in the upper part of the section. They are interpreted as derived mainly from high temperature quartz of plutonic/volcanic origin. No internal feature of detrital quartz is found. In molasse sequence, quartz CL population seems to be similar to flysch sequence but represents more various quartz provenances (Fig. 6). CL characteristic of internal quartz grain such as zoned, mottled, and streak structure is well presented.

## PROVENANCE AND TECTONIC DISCUSSIONS

From the result of major and trace elements analysis, the deposition of the Nam Duk Basin started from pelagic sequence which was formed in deep sea environment of an oceanic island arc setting. The source of the detritus was from metabasic provenance. Trace elements characteristics indicate that the chemical composition of pelagic is different from those of flysch and molasse sediments. However, siliciclastic sediments of flysch and molasse sequences are similar to those deposited in a continental island arc setting. The provenance is considered to be from mafic igneous, metabasic, and probably some granitic gneiss sources. In addition, this result proved that the Nam Duk Basin was transitional from oceanic to continental island arc environment.

From the results of CL analysis, during Lower to

Middle Permian, sediments of metamorphic terrane provenance were supplied into the Basin. Input of detrital quartz grains were dominantly contributed by volcanism and/or plutonism activity as indicated by the blue CL quartz. The result is consistent with the occurrence of dacitic to rhyodacitic tuffite layer interbedded with allodapic limestones of pelagic sequence<sup>4</sup>. The derivation of detrital quartz can be explain by transported of sub-aerial volcanism along the basin axis<sup>4</sup> or on a land area west of the Phetchabun region or from volcanic islands within the geosynclines<sup>31</sup>. Therefore, it can be concluded that detrital quartz in pelagic basin was not denuded from a metamorphic terrane. It was derived from volcanic source in the basin and was probably from the west as mentioned by Bunopas and Vella<sup>31</sup>. Flysch samples clearly show low variety of volcanic and/or plutonic provenance especially in the lower part of the section which is dominated by brown luminescence. Most of brown CL detrital grains are interpreted to be derived from regional low-grade metamorphic region. Some of them clearly show crystalline texture and are derived from thermally metamorphosed quartz at low temperature. A minor blue luminescence quartz grains are interpreted as derived mainly from plutonic/volcanic complex during suturing. They are more prominent in the upper part of the section.

In molasse sequence, quartz CL population seems to be similar to flysch sequence but represents more variety of quartz provenances. CL characteristic of quartz grain such as zoned, mottled, and streak structure is present and it indicates metamorphic, hydrothermal, volcanic, and plutonic provenance. High population of detrital quartz family in molasse sequence especially the sample no. 40+400 is remarkable and it is important for tectonic interpretation. Based on sedimentological characteristic, molasse is less deformed than flysch strata and graded into shallow marine environment<sup>8</sup>. Thus, interpretation of post-orogenic event for molasse sequence is consistent with the continuous supply of siliciclastic sediments from the same mountain range of flysch strata until suturing. The molasses also contains detritus derived from highland plutonic/volcanic rock probably rhyolitic and recycled sediments from the older rocks.

The discovery of detrital chromian spinels in the flysch and molasse sequences of the Nam Duk Formation was reported by Chutakositkanon et al.<sup>32,33</sup>. However, interpretation of the provenance of the chromian spinels from the Loei – ultramafic located in eastern edge of Nam Duk Basin is unlikely and inconsistent with the geologic evolution of the region<sup>34,35</sup>. The present study confirms that the sources of the chromian spinels is likely to be derived from the

ultramafic accreted to the subduction complex in the west. This provenance contributed the siliciclastic sediments of flysch and molasse sequences including detrital chromian spinels.

The sandstone samples from Chiang Khan (Middle-Late Permian “Pha Dua Formation”) display mainly detrital quartz grains derived from metamorphic sources<sup>10</sup>. This could be related to the denudation of metamorphic terrane on the east of the Nam Duk Basin. The metamorphic source is interpreted as derived from the older orogen deformed during Late Devonian-Early Carboniferous (Intasopa and Dunn, 1994). Comparisons of geochemical and cathodoluminescence

characteristic of the sections north and south of the Nam Duk Formation at its type section have been done by Malila (2005). The result shows that the Tha Li siliciclastic sediments approximately 150 kilometers north of Lom Sak and the Pang Asok Formation in the Saraburi region to the south can be correlated with the flysch and/or molasse sequences. This indicates that the axis of the Nam Duk Basin is at least 400 kilometers long in an N-S direction along the western margin of the Khorat Plateau. Detail of stratigraphic succession and provenance and tectonic setting of the Nam Duk Formation is given in Figure 7a.

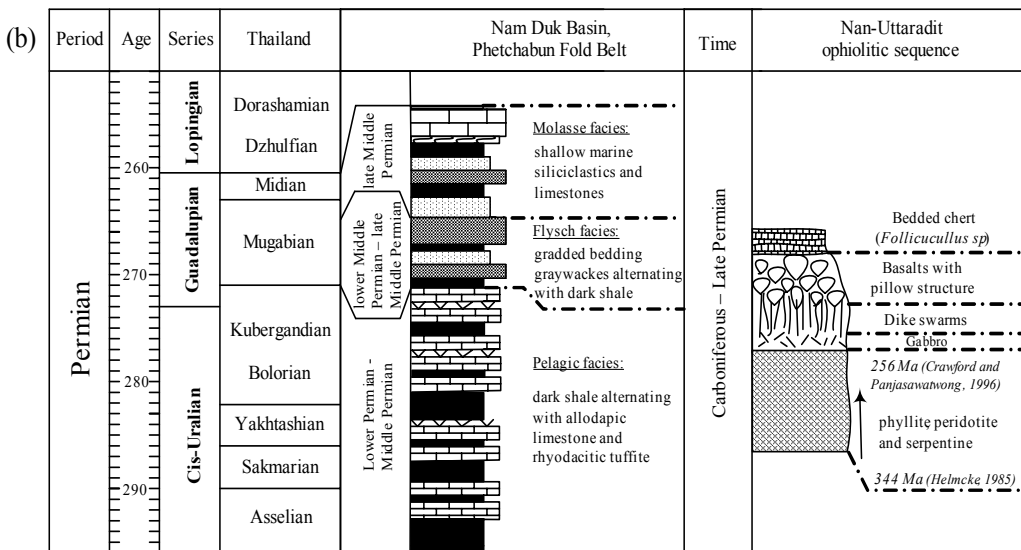
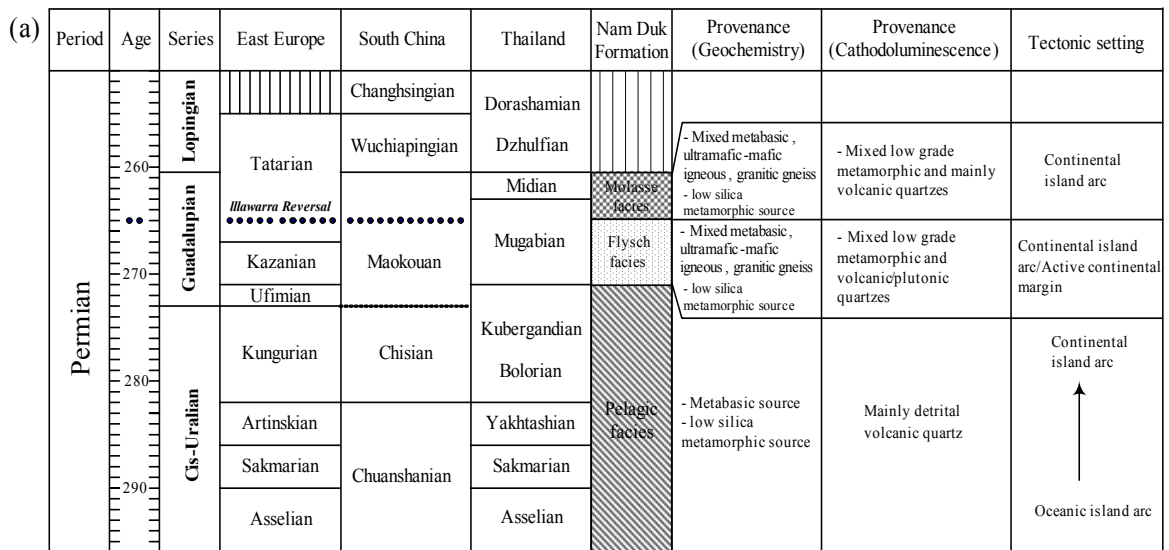


**Fig 7.** (a) Detailed stratigraphic succession of the Nam Duk Formation including its provenance and tectonic setting based on geochemical and cathodoluminescence data. (b) Idealized vertical sequence from ophiolite suite of Nan-Uttaradit suture zone and the Nam Duk Basin during Late Paleozoic.

## GEODYNAMIC EVOLUTION OF THE NAM DUK BASIN

From geochemical and cathodoluminescence results including the published data from various authors, the possible evolution and paleotectonic reconstruction of the Nam Duk Formation are summarized as following.

The Nam Duk Basin was formed as a back arc basin after the closure of small oceanic basin (Loei Ocean) in Indosinia continent during the Devonian-Carboniferous<sup>36</sup>. This basin rifting probably occurred in Middle Carboniferous<sup>37</sup> and subsequently the pelagic sediments were accumulated during Middle – Late Carboniferous to lower Middle Permian in a deep sea basin. This deep sea oceanic basin was bordered on both sides by shallow marine sea. The geochemical and cathodoluminescence results indicate that the pelagic facies of a deep sea basin was formed close to an oceanic island and on an oceanic crust.

The Pha Nok Khao and the Khao Khwang Platforms (or probably one coherent unit) were located in the eastern side of the Nam Duk Basin or the western margin of the Indochina plate. The subduction of Indochina beneath the Shan-Thai cratons (on the west) towards west was started in the late Middle Permian. During subduction the accretionary complex comprising mixture of pelagic sediments including radiolarian chert and mafic-ultramafic rocks was formed at the eastern margin of the Shan-Thai block. This ophiolite belt has been known as the Nan-Uttaradit Suture Zone. Erosion of the accretionary complex produced the influx of siliciclastic or flysch sediments to the Nam Duk Basin. The provenance signature of the flysch sequence shows the mafic igneous source which is interpreted as being derived from the accretionary complex.

The result of geochemical analysis of flysch sequence as discussed earlier indicates that it was deposited in a continental island arc setting and it was in an outer or a fore-arc environment. Upon the oceanic crust was completely consumed the Indochina collided with the Shan-Thai terranes causing the Late Variscan Orogeny<sup>3</sup>. The basin was shallowing, the siliciclastic sediments were continuously supplied from the same sources representing the molasse sediments. The geochemical and cathodoluminescence results confirm that both flysch and molasse sequences show similar characteristics representing the same provenance and tectonic setting. However, the molasse contains more volcanic quartz grains than flysch and more recycled sediments.

Correlation of the Late Paleozoic strata in the Nan-Uttaradit suture zone and the Phetchabun Fold Belt reveals a continuous sedimentary sequence which can be used for the paleotectonic reconstruction. Figure

7b displays an idealized vertical sequence from oceanic igneous rocks and chert (ophiolite sequence) passing upward through pelagic, greywacke (flysch or turbidite) to shallow marine clastic (molasse) deposits. The vertical sequence can be explained by the process of seafloor spreading. The oceanic crust (pillow basalt, gabbro, and peridotite) was formed by the rifting and was followed by chert sequence in Nan and part of the pelagic facies in the Nam Duk Basin. These were subsequently followed by turbiditic limestone and flysch sedimentation in a remnant ocean basin. After the remnant ocean was closed, a peripheral foreland basin was formed with molasse sedimentation. The changing of flysch to molasse sediments as the result of the termination of the oceanic basin indicates the maximum deformation or disturbance which is known as the Late Variscan Orogeny<sup>3,38</sup>.

A geodynamic model based on geochemical and cathodoluminescence analysis is shown in Figure 8.

## CONCLUSIONS

Provenance study of the siliciclastic sediments in the Nam Duk Formation has been done based on geochemical and cathodoluminescence analysis. The geodynamic evolution of the Nam Duk Basin and Phetchabun Fold Belt is proposed and discussed. The results can be summarized as follows;

1. The pelagic sequence of the Nam Duk Formation was formed in an oceanic setting between oceanic island and continental island arc environments. The source of the quartz detritus in the allodapic limestone was from metabasic and volcanic provenance.

2. The flysch and molasse sequences show similar geochemical characteristics (very high  $\text{TiO}_2$  and  $\text{Fe}_2\text{O}_3$ , low  $\text{Al}_2\text{O}_3$ ) and indicate mixed mafic igneous, metabasic, granitic gneiss, and low-silica metamorphic sources. Both sequences were deposited in a continental island arc setting.

3. Tectonically, subduction of the Indochina beneath the Shan-Thai cratons (on the west) towards west was started in the late Middle Permian resulting in the formation of an accretionary complex. The provenance signature of the flysch sequence shows the mafic igneous source which is interpreted as being derived from the accretionary complex and it was in an outer or a fore-arc environment. The maximum orogenic movement occurred during the completion of suturing process. The molasse sequence consisting predominantly of the siliciclastic sediments was accumulated after mountain building process.

4. This study supports an idea of Nan-Uttaradit suture as being one branch of the main Paleo-Tethys represented by the remnant ocean known as the Nam Duk Basin in the Phetchabun Fold Belt. This ocean was

already closed during the short period of Middle Permian.

**ACKNOWLEDGEMENTS**

We gratefully thank the Royal Golden Jubilee Ph.D. Program (RGJ No. PHD/0140/2545), Thailand Research Fund, and the DAAD of Germany for the financial support throughout this research. Special thanks are also extended to the Suranaree University of Technology

(Thailand), the University of Göttingen (Germany), and the China University of Geosciences (Wuhan, China). The bulk of the work presented here was undertaken whilst Kitsana M was a PhD candidate at the Suranaree University of Technology.

**REFERENCES**

1. Bunopas, S (1981) Paleogeographic history of western Thailand and adjacent parts of Southeast Asia: A plate

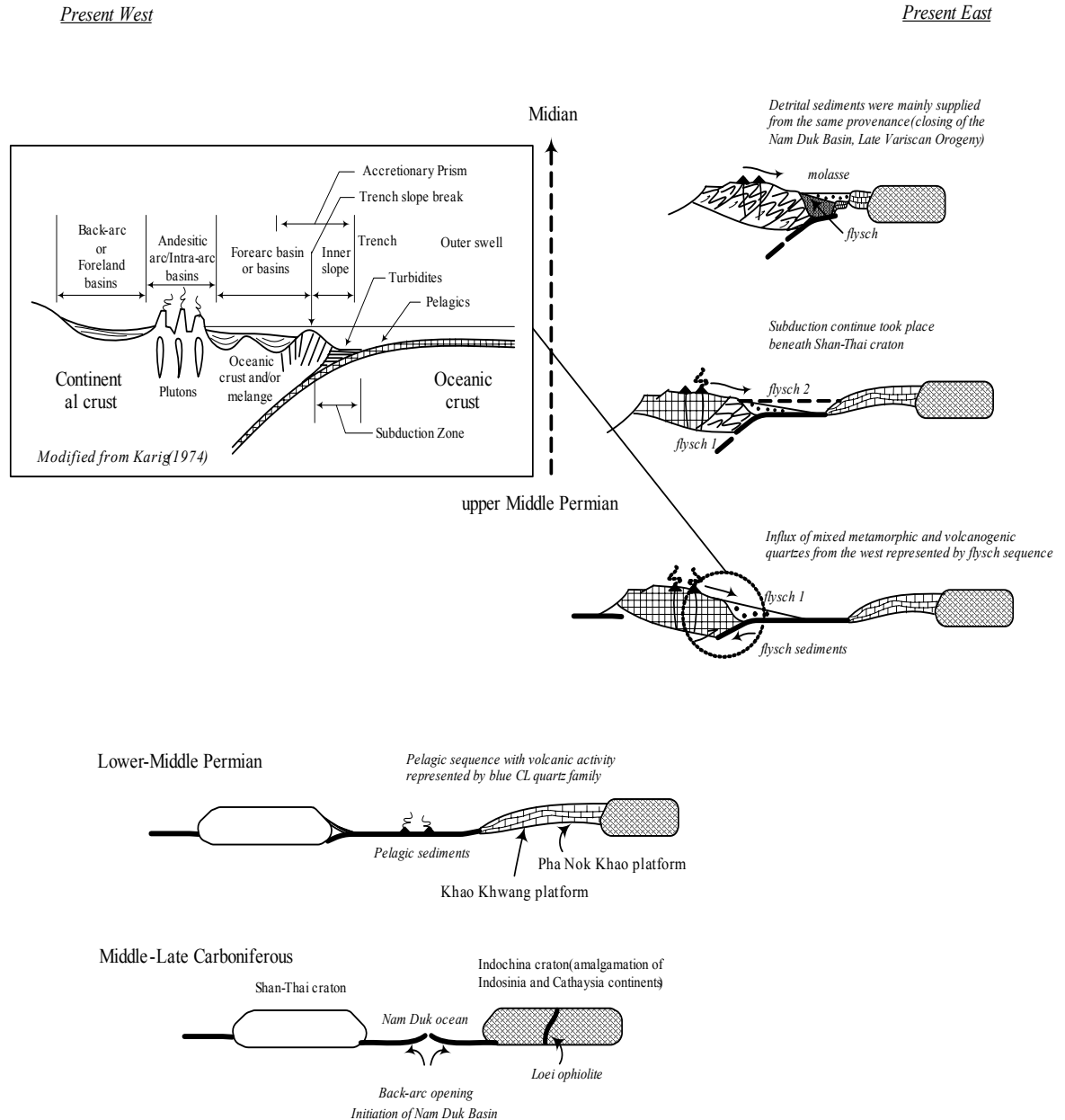


**Fig 8.** Tectonic model and evolution of the Nam Duk Basin and adjacent region during Late Paleozoic - Triassic based on geochemical and cathodoluminescence analysis including data from various publications.

- tectonics interpretation. Ph.D. Dissertation, Victoria University of Wellington, New Zealand. Reprinted 1982 as Geological Survey Paper 5, Department of Mineral Resources, Bangkok, Thailand.
2. Helmcke, D and Kraikhong, C (1982) On the geocynclinal and orogenic evolution of central and northeastern Thailand. *Journal of Geological Society of Thailand* **5**, 52-47.
  3. Helmcke, D and Lindenberg, H G (1983) New data on the Indosinian orogeny from Central Thailand. *Geologische Rundschau* **72**, 317-28.
  4. Winkel, R, Ingavat, R and Helmcke, D (1983) Facies and stratigraphy of the Lower-Lower Middle Permian strata of the Phetchabun Fold-Belt in Central Thailand. Workshop on stratigraphic correlation of Thailand and Malaysia. Haad Yai, 8-10 September. Thailand, 293-306.
  5. Ingavat-Helmcke, R and Helmcke, D (1986) Permian Fusulinacean Faunas of Thailand – Event Controlled Evolution. *Lecture Notes in Earth Sciences* **8**, 241-8.
  6. Chonglakmani, C and Sattayarak, N (1978) Stratigraphy of the Huai Hin Lat Formation (Upper Triassic) in northeastern Thailand. In: Proc GEOSEA III (Edited by Nutalaya P) Bangkok, Thailand, 739-762.
  7. Wielchowsky, C C and Young, J D (1985) Regional facies variations in Permian rocks of the Phetchabun fold and thrust belt, Thailand. Conference on the Geology and Mineral Resource Development of NE Thailand, Khon Kaen University, 41-55.
  8. Altermann, W, Grammel, S, Ingavat, R, Nakornsri, N and Helmcke, D (1983) On the evolution of the Paleozoic terrains bordering the Northwestern Khorat Plateau. Conference on Geology and Mineral Resources of Thailand. Department of Mineral Resources, Bangkok, November. preprint 5 p.
  9. Charoentitirat, T (2002) Permian fusulinodean biostratigraphy and carbonate development in the Indochina Block of Thailand with their paleogeographic implication. Doctoral Thesis, University of Tsukuba, Japan.
  10. Malila, K (2005) Provenance of the Nam Duk Formation and Implications for the Geodynamic Evolution of the Phetchabun Fold Belt. Ph.D. Thesis, Suranaree University of Technology, 126 p.
  11. Bhatia, M R (1983) Plate tectonics and geochemical composition of sandstones. *Journal of Geology* **91**, 611-627.
  12. Roser, B P and Korsch, R J (1986) Determination of tectonic setting of sandstone-mudstone suites using SiO<sub>2</sub> content and K<sub>2</sub>O/Na<sub>2</sub>O ratio. *Journal of Geology* **94**, 635-690.
  13. Maynard, J B (1992) Chemistry of modern soils as a guide to interpreting Precambrian paleosols. *Journal of Geology* **100**, 279-289.
  14. Young, G M and Nesbitt, H E (1999) Paleoclimatology and provenance of the glaciogenic Gowganda Formation (Paleoproterozoic), Ontario, Canada: a chemostratigraphic approach. *Geological Society of America* **111**, 264-274
  15. Roser, B P and Korsch, R J (1988) Provenance signature of sandstone-mudstone suites determined using discriminant function analysis of major element data. *Chemistry Geology* **67**, 119-139.
  16. Bhatia, M R and Crook, K A W (1986) Trace element characteristics of graywackes and tectonic discrimination of sedimentary basins. *Contrib. Mineral Petrol* **92**, 181-193.
  17. McLennan, S M, Hemming, S, McDaniel, D K and Hanson, G N (1993) Geochemical approaches to sedimentation, provenance, and tectonics, *Geological Society of America Special paper* **284**, 21-41.
  18. Andre, L, Deutsch, S and Hertogen, J (1986) Trace-element and Nd isotopes in shales as indexes of provenance and crustal growth: The early Paleozoic from the Brabantmassif (Belgium). *Chemical Geology* **57**, 101-115.
  19. Cullers, R L, Basu, A and Suttner, L (1988) Geochemical signature of provenance in sand-size material in soils and stream sediments near the Tobacco Root Batholith, Montana, U.S.A. *Chemical Geology* **70**, 335-348.
  20. Cullers, R L (1994) The chemical signature of source rock in size fractions of Holocene stream sediment derived from metamorphic rocks in the Wet Mountains region, Colorado, U.S.A. *Chemical Geology* **113**, 327-343.
  21. Bhatia, M R (1985) Rare earth element geochemistry of Australian Paleozoic graywackes and mudrocks: Provenance and tectonic control. *Sedimentary Geology* **45**, 97-113.
  22. Neuser, R D, Bruhn, F, Götze, J, Habermann, D and Riegter, D K (1995) Kathodolumineszenz: Methodik und Anwendung. *Zbl. Geol. Paläont. Teil 1 (1/2)*, pp 287-306.
  23. Owen, M R (1991) Application of cathodoluminescence to sandstone provenance. In: SEPM Short Course 25 (Edited by Barker C E and Kopp O C), 67-75.
  24. Zinkernagel, U (1978) Cathodoluminescence of quartz and its application to sandstone petrology. *Contrib to Sediment* **8**, Stuttgart E Schweizer Verlag, 69 p.
  25. Götze, J and Simmerle, W (2000) Quartz and silica as guide to provenance in sediments and sedimentary rocks. *Contrib Sediment Geol* **12**, 1-91.
  26. Müller, A (2000) Cathodoluminescence and characterization of defect structures in quartz with application to the study of granitic rocks. Ph.D. Thesis, University of Göttingen, 229 p.
  27. Seyedolali, A, Krinsley, D H, Boggs, S, Ohara, P F, Dypvik, H and Goles, G G (1997) Provenance interpretation of quartz by scanning electron microscope-cathodoluminescence fabric analysis. *Geology* **25**, 787-790.
  28. Kwon, Y I and Boggs, Jr S (2002) Provenance interpretation of Tertiary sandstones from the Cheju Basin (NE East Chian Sea): a comparison of conventional petrographic and scanning cathodoluminescence techniques. *Sedimentary Geology* **152**, pp 29-43.
  29. Herron, M M (1988) Geochemical classification of terrigenous sands and shales from core or log data. *Journal of Sedimentary Petrology* **58**, 820-829.
  30. Hiscott, R N (1984) Ophiolitic source rocks for Taconic-age flysch: trace element evidence. *Geological Society of America Bulletin* **95**, 1261-1267.
  31. Bhatia, M R (1985) Rare earth element geochemistry of Australian Paleozoic graywackes and mudrocks: Provenance and tectonic control. *Sedimentary Geology* **45**, 97-113.
  32. Bunopas, S and Vella, P (1978) Late Paleozoic and Mesozoic structural evolution of Northern Thailand: A plate tectonic model. In: Proc GEOSEA III (Edited by Nutalaya P) Bangkok, Thailand, 133-140.
  33. Chutakositkanon, V, Hisada, K, Uneo, K and Charusiri, P (1997) New suture and terrane deduced from detrital chromian spinel in sandstone of the Nam Duk Formation, north-central Thailand: preliminary report. In: Proceedings of the international conference on stratigraphy and tectonic evolution of Southeast Asia and the South Pacific (Edited by Dheeradilok P et al), Department of Mineral Resources, Bangkok Thailand, 366-8
  34. Chutakositkanon, V, Hisada, K, Charusiri, P, Arai, S and Charoentitirat, T (1999) Characteristics of detrital chromian spinels from the Nam Duk Formation: Implication for the occurrence of mysterious ultramafic and volcanic rocks in central Thailand. In: Symposium on Mineral, Energy, and Water Resources of Thailand: Towards the year 2000 (Edited by Khantaprab C et al), Chulalongkorn University, Thailand, 604-6.
  35. Chonglakmani, C and Helmcke, D (2001) Geodynamic

- evolution of Loei and Phetchabun regions; Does the discovery of detrital chromian spinels from the Nam Duk Formation (Permian, north-central Thailand) provide new constraint?. *Gondwana Research* **4(3)**, 437-42.
35. Chonglakmani, C, Qinglai, F, Meischner, D, Ingavat-Helmcke, R and Helmcke, D (2001) Correlation of tectono-stratigraphic units in northern Thailand with those of western Yunnan (China). *Journal of China University of Geosciences* **12(3)**, 207-13.
  36. Intasopa, S. and Dunn, T (1994) Petrology and Sr-Nd isotopic systems of the basalts and rhyolites, Loei, Thailand. *Journal of Southeast Asian Earth Sciences* **9**, 167-80.
  37. Kozar, M G, Crandall, G F and Hall, S E (1992) Integrated Structural and Stratigraphic Study of the Khorat Basin, Ratburi Limestone (Permian), Thailand. In: Proceeding of the national conference on the geologic resources of Thailand: Potential for future development (Edited by Piancharoen C), Department of Mineral Resources, Bangkok, Thailand, 692-736.
  38. Helmcke, D (1985) The Permo-Triassic "Paleotethys" in Mainland Southeast-Asia and adjacent parts of China. *Geologische Rundschau* **74/2**, 215-28.